

CRATER SHAPE EVOLUTION WITH LATITUDE IN TERRA CIMMERIA, MARS – IMPLICATIONS FOR CLIMATE. S. J. Conway¹, N. Mangold¹ and V. Ansan¹, ¹LPGN, CNRS/Univ. Nantes, 44322 Nantes, France, susan.conway@univ-nantes.fr.

Introduction: We have used topographic data from the High Resolution Stereo Camera (HRSC) in the Terra Cimmeria region on Mars running from latitudes 25 to 50°S (Fig. 1) to investigate the effects of climate on changing crater form. The Mars Orbiter Laser Altimeter (MOLA) global topographic data have already revealed that steep slopes are more prevalent near the equator and that gradual softening of topography occurs towards the poles [1] due to deposition of a volatile-rich ‘mantling’ material [2]. We have taken advantage of the higher resolution of the HRSC data (30-90 m/pix in the 5 HRSC DEMs used compared to ~400 m/pix for MOLA) to investigate whether similar trends can be seen in crater shape.

Approach: We used crater survey GT57633 [3] as a basis for our extended crater map in this region. For each crater we delineated four zones: north-, south-, east- and west-facing (Fig. 2). Within each zone we calculated the curvature of the crater wall, its mean slope and its maximum slope. The process is illustrated in Fig. 2. This was achieved by averaging all data points in 100m distance intervals from the centre-point. The maximum and mean slopes were calculated from these profiles. For each profile the distance from the centre-point was normalized by the crater radius and the height was normalized by overall crater depth. A power-law of the form $y = Ax^n$ was fitted to the normalized data. The exponent n of the power law describes the curvature of the crater walls, low values being bowl-shaped and high values being flat-bottomed, or U-shaped. We also performed a rudimentary classification of craters into ‘young’, those with visible ejecta and sharp rim, and otherwise ‘old’.

We compared results from our 30 and 90 m HRSC elevation models, to those from MOLA gridded data at ~400m resolution.

Results: We measured 433 craters ranging from 1 to 64 km in diameter in the region. The exponent of the power law (n) increases towards higher latitudes and this is more marked for south-facing slopes. This trend is almost undetectable in MOLA data. This implies craters become more ‘U’ shaped, or flat-bottomed rather than bowl-shaped towards the pole. This trend is less marked in ‘young’ craters. We attribute this to the greater infilling of craters at mid-latitudes, possibly associated with viscous flow features [4]. We have not noted any particular trend for the coefficient of the power law (A).

We observed that steeper maximum slopes are found towards the equator, as expected from previous work [1]. This trend is present in MOLA gridded data, but not as strong as for HRSC, or the MOLA profile data used by [1]. This trend is stronger for south- or pole-facing slopes (Fig. 3) and for ‘young’ craters in the HRSC data. It is also noteworthy that the slopes measured in HRSC data are much higher than those measured from MOLA (mean of 0.07 in MOLA and 0.26 in HRSC).

Mean slope shows a similar latitudinal trend to the maximum slope, but south-facing slopes and young craters are not different from the general population.

Conclusions and outlook: The trends for crater shape are clearer in HRSC data than for MOLA gridded data. The HRSC data can be used to study slopes of any orientation, unlike MOLA profile data, which can only be used in the N-S direction. Hence, HRSC data presents a better candidate for regional studies of topography. We have found crater shape is highly dependent on latitude, with steeper slopes and bowl-shaped forms being more common towards the equator in slopes of all orientations, and particularly pole-facing ones. We intend to map gullies and viscous flow features, which are climate-related features, to assess their influence on these trends in crater form. We will also utilize landscape evolution models to evaluate the effects of different slope processes (e.g. creep, rockfall, gullying).

References: [1] Kreslavsky M. A. and Head J. W. (2000) *JGR*, 105, 26695-26712. [2] Mustard J. F. et al. (2001) *Nature*, 412, 411-414. [3] Salamunićar G. and Lončarić S. (2008) *PSS*, 56, 1992-2008. [4] Milliken R. E. et al. (2003) *JGR Planets*, 108, doi:10.1029/2002JE002005.

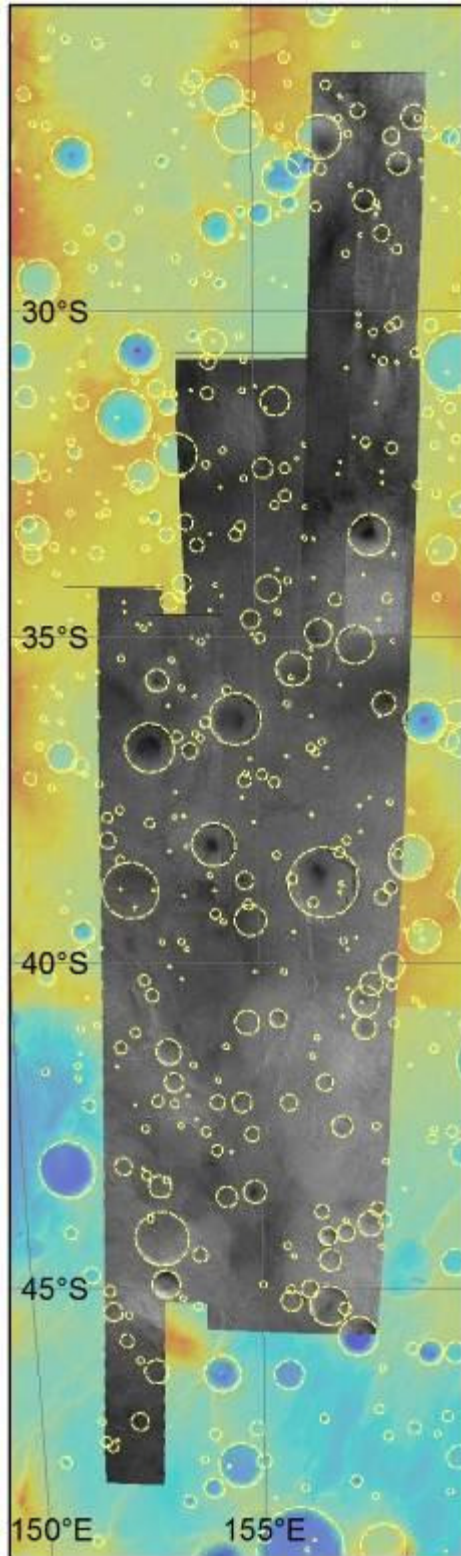


Fig. 1. Map of study area, with craters marked in yellow, background is MOLA, and images are HRSC H0228_0000, H0241_0000, H0280_0001, H0293_0000 and H2590_0001.

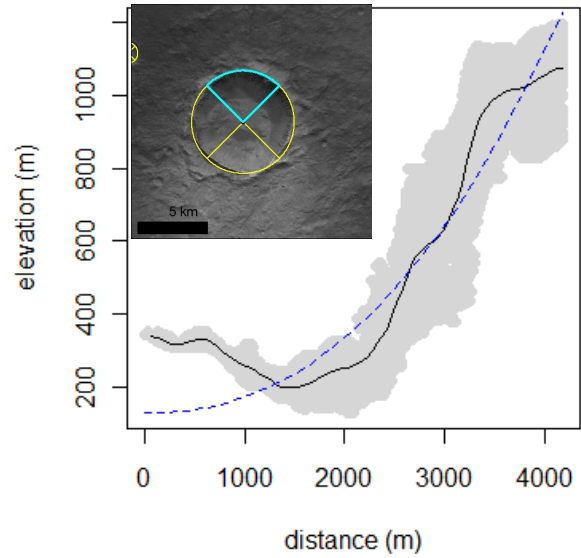


Fig. 2. Illustration of procedure to extract statistics from craters. The elevation data within the blue segment highlighted in the insert graphic are plotted in grey on the graph. The black line is the average slope profile for these data, from which the maximum slope is calculated. The dotted blue line is the power-law fit (un-normalized to aid display).

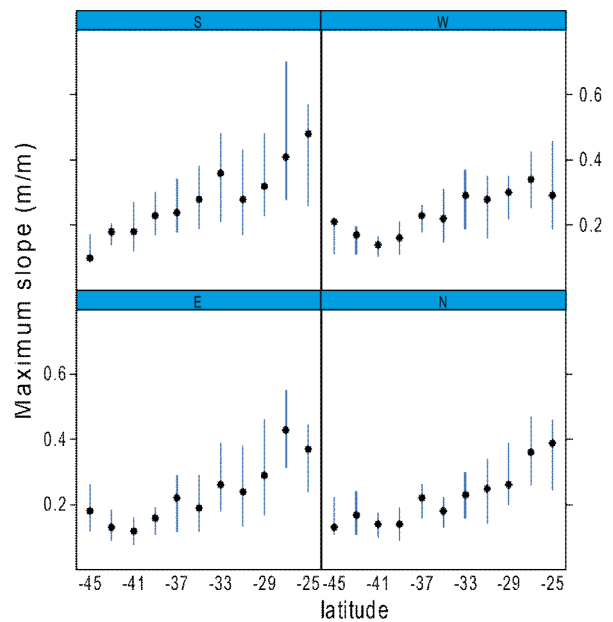


Fig. 3. Maximum crater wall slope against latitude for S-, W-, E- and N-facing slopes. Dots are means and blue bars are one standard deviation.